Temperature effect on the steric and polar Taft substituent parameter values

Sindi Baco, Marcel Klinksiek, Melanie Mignot, Christoph Held, Julien Legros, Sébastien Leveneur

Temperature effect on the steric and polar Taft substituent parameter values

Sindi Baco[a,b,c] Marcel Klinksiek,[b] Mélanie Mignot,[c] Christoph Held,[b] Julien Legros,[c] and Sébastien Leveneur[a*]

[a.] *INSA Rouen Normandie, UNIROUEN, Normandie Univ, LSPC, UR4704, F-76000 Rouen, France, France*

[b.] *Laboratory of Thermodynamics, Department of Biochemical and Chemical Engineering, TU Dortmund University, Emil-Figge. Str.70, 44227 Dortmund, Germany*

[c] *INSA Rouen Normandie, Univ Rouen Normandie, CNRS, Normandie Univ, COBRA UMR 6014, INC3M FR 3038, F-76000 Rouen, France*

The concept of Linear Free-Energy Relationships (LFER) is applied in different fields of chemistry, such as toxicology or kinetics. The knowledge of reactivity from the reactant structure can aid biomass valorization processes by decreasing the number of experiments to carry out in the kinetic modeling stage. The Taft equation, based on LFER, represents a link between the kinetics and the structure of the species involved in the reaction, by quantifying polar, steric and resonance effects, also known as Taft substituent parameters. This equation was used in different reaction systems in different studies, but none considered the influence of temperature on the steric and polar Taft substituent parameters. In this work, we investigated this aspect by re-evaluating the substituent parameters of Taft equation applied to the esterification of levulinic acid by methanol and ethanol, and the saponification of methyl and ethyl levulinates. Levulinic acid was chosen because it is a promising platform molecule. We found that the Taft substituent parameters are relatively sensitive to temperature and vary linearly within the same temperature range, the steric effect decreases by almost double while the polar effect grows less significantly.

1 Introduction

Developing sustainable, safe and environmentally friendly processes is crucial for modern society. Using biomass materials, particularly lignocellulosic biomass (LCB), as raw materials can contribute to this development.[1–3] LCB is made of cellulose and hemicellulose, which are sugar polymers and lignin aromatic polymers. The valorization of the sugar fraction, namely cellulose and hemicellulose, leads to the production of several platform molecules such as levulinic acid or levulinates, furfural, 5-hydroxymethylfurfural (5-HMF) or its etherified forms 5-alkoxymethylfurfural (5-RMF), glycerol, etc.[4–8]

Chemical valorization of these sugar fractions raises several questions on which catalyst to use, which solvent to select, and which models to describe the kinetic and thermodynamic phenomena in a reliable way. For instance, the production of 5-HMF or 5-RMF is from the solvolysis of simple sugars using water (H-OH) or alcohol solvent (R-OH).[7] The hypothesis that there is a relationship between the alcohol reactivity and its substituent -R can reduce the experimental stage. Indeed, one can study one alcohol and predict the reactivity of other alcohols via the relationship.

The link between reactant structure and reactivity can be considered as an old quest. In the 30's, Evans and Polanyi derived the concept of Linear Free Energy Relationships (LFER) based on the assumption that there is a linear relationship between the activation free energy and the Gibbs free energy of the reaction.[9–12] In a series of closely related atom-transfer reactions, they concluded that the activation energy varies linearly with the reaction enthalpy.

One should also mention Sterimol parameters developed by Verloop[13–16] that evaluate the steric effect by considering the different spatial subparameters linked to the conformation of the –R group and the overall interactions between the reactants.

The concept of LFER has led to several equations that quantifies the structure-reactivity parameters experimentally, such as : Hammett,[17] Taft[18–23], Charton,[24–27] Grunwald–Winstein, Swain–Lupton equations. These semi-empirical equations assume a relationship between the substituents (-R) attached to a functional group and its reactivity in a series. This approach can only be done for a congeneric series of compounds, meaning sets of compounds that share the same functional group or reaction center Y (like –COOH, -SH, -NH_2, -CO) and have only variations in the substituent -R attached to this functional group or reaction center (Fig. 1).

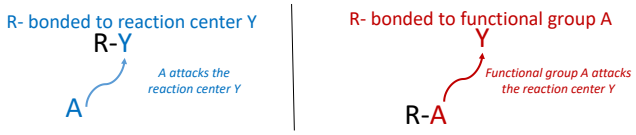

Fig. 1 Reactivity when -R is attached to reaction center Y and when -R is attached to the functional group A.

Predicting thermodynamic and kinetic behavior from reactant structure was a breakthrough in chemistry and kinetics.[28–33] The effects of the substituents (-R) on the reaction center or functional groups are caused by polar, resonance, and steric effects. For that reason, the different equations based on LFER consider these effects.

In 1937, Hammett[34,35] quantified the effects of the substituent in meta- and para- position in benzene structure on ester hydrolysis. Taft[19–23] extended this approach to aliphatic derivatives and ortho-substituted aromatic compounds where steric effects are essential. Taft proposed the following equation derived from LFER concept:

$$\log\frac{k_{-R}(T)}{k_{-Me}(T)} = \rho^* \cdot \sigma^*(-R) + \delta \cdot E_s(-R) + \Psi \qquad (1)$$

- $k_{-R}(T)$ is the rate constant at a temperature T of a reaction involving the substituent $-R$ and $k_{-Me}(T)$ is the rate constant at the same temperature T of the same reaction but involving the reference substituent, which is the methyl group (CH_3-) for Taft equation.
- $\sigma^*(-R)$ represents the net polar effect of the substituent $-R$ on the functional group or reaction center. It measures the inductive electron-withdrawing or –donating toward the functional group or reaction center. From the literature, it only depends on the nature of $-R$.
- ρ^* is a constant measuring the importance of the polar effect on a given reaction series. From the literature, its value can depend on several operating conditions, such as the nature of the reaction center or functional group and temperature.
- $E_s(-R)$ represents the total steric effect due to the substituent $-R$ on the functional group or reaction center. From the literature, it only depends on the nature of $-R$.

- δ is a constant value evaluating the importance of steric effect for a given reaction series. This value depends also on the nature of the reaction center/functional group and temperature.
- Ψ is a parameter considering the resonance effect between the substituent and the reaction center.

$E_s(-R)$ and $\sigma^*(-R)$ depend on the substituent and are named Taft substituent parameters; whereas ρ^* and δ characterize the reaction kinetics and are named Taft reaction parameters.

For the evaluation of $E_s(-R)$ and $\sigma^*(-R)$, Taft used the rates of ester hydrolysis (saponification) and carboxylic acid esterification. He derived eqn (2) and (3):

$$\left(\log\frac{k_{-R}(T)}{k_{-Me}(T)}\right)_A = E_s(-R) \quad (2)$$

$$\sigma^*(-R) = \frac{1}{2.48}\cdot\left[\left(\log\frac{k_{-R}(T)}{k_{-Me}(T)}\right)_B - \left(\log\frac{k_{-R}(T)}{k_{-Me}(T)}\right)_A\right] \quad (3)$$

- Subscripts B and A refer to basic and acidic reactions, respectively,
- Factor 2.48 is a constant introduced to put the estimated polar effects on about the same scale as for the ones of Hammett scale.

The values of $\sigma^*(-R)$ and $E_s(-R)$ for different substituents is textbook knowledge. As noticed by MacPhee et al.,[36] Dubois et al.[37] and Panaye et al.[38], the original values were measured at diverse conditions. Thus, they revisited and unified $E_s(-R)$ by choosing as reference reaction the acid catalyzed esterification of carboxylic acids in methanol solvent at 40°C. Strictly speaking, these parameters should only be used for reactions in methanol solvent at 40°C. In these previous research papers, kinetic models were not developed, and rate constants were globally evaluated from initial reaction rates. One should also mention the work of Brändström[39] and Neuvonen et al.[40] to predict the values of $\sigma^*(-R)$, but they did not include the effect of temperature.

Recently, the application of Taft equation has been successfully tested for different reaction systems: esterification over homogeneous catalyst,[41,42] esterification over heterogeneous catalyst,[43] alkoxysilanes hydrolysis,[44] carboxylic acid perhydrolysis [45] and epoxidation of vegetable oils.[46] In 2019, Wang et al.[47] demonstrated that hydrogenation of levulinic acid and its esters follows Taft equation, but a simplified kinetic model based on power law was used.

To the best of our knowledge, there is a lack of investigation concerning the dependence of $\sigma^*(-R)$ and $E_s(-R)$ on the reaction temperature. The objective of this study is to fill this gap via the development of reliable kinetic models, including the proton catalytic effect and reaction equilibrium. Such investigation is also missing in the use of Sterimol parameters.

In this manuscript, the acid esterification of levulinic acid by methanol and ethanol was studied to evaluate $E_s(-R)$ and the basic saponification of methyl and ethyl levulinate was studied to evaluate $\sigma^*(-R)$. For all these chemical systems, kinetic models were developed to determine the impact of temperature on the Taft substituent parameters, and water was used as a solvent. Levulinic acid choice was motivated because it is the starting material of several reactions.[48–52] Both reaction are displayed in Fig. 2 & Fig. 3:

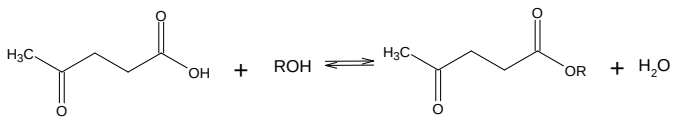

Fig. 2 Levulinic acid esterification reaction.

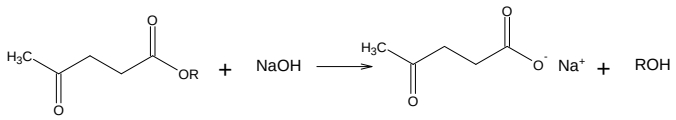

Fig. 3 Alkyl levulinates saponification in NaOH aqueous environment.

2 Experimental

2.1 Chemicals

The following chemicals were used without further purification: levulinic acid (LA) (wt% >= 97%) purchased from Sigma Aldrich. Ethanol absolute (EtOH) (wt% >= 99.7%), methanol absolute (MeOH) (wt% >= 99.7%) and acetone (wt% 99.8 vol%) were supplied by VWR Chemicals. Ethyl levulinate (EL) (wt% >= 98%) and methyl levulinate (ML) was purchased from Acros Organics. Sulfuric acid (wt% >= 98%) was obtained from Honeywell Fukla Chemicals. Finally, sodium hydroxide pellets was purchased from Panreac. Distilled water (W) was used.

2.2 Procedure

All experiments were carried out in isothermal conditions. Esterification reactions were carried out in a glass reactor vessel, operating in batch mode at atmospheric pressure. It was equipped with a jacket, where water was used to heat the system via a thermostat. To avoid any loss of mass caused by the evaporation, a condenser with water circulating was present and fixed at 15°C. A mechanical stirrer, fixed at 450 rpm, is also present to guarantee a homogeneous reaction mixture.

Saponification reactions were carried out in a glass reactor vessel, operating in batch mode at atmospheric pressure, similar to the previous one. It was equipped with a heated jacket, a reflux condenser, a mechanical stirrer fixed at 450 rpm and a conductivity probe.

During the esterification reactions, samples were taken at different time intervals using a plastic syringe. During the saponification reactions, the conductivity value was recorded online.

In the esterification kinetic experiments, starting solutions with only one reactant were poured into the reactor, and the temperature was brought to the desired reaction temperature before adding the preheated second reactant. The starting solution was a mixture of water and alcohol, while the preheated second reactant was an aqueous solution of LA (or EL or ML) and H_2SO_4.

In the saponification kinetic experiments, a known quantity of solid NaOH was dissolved in water and poured into the reactor and the temperature was brought to the desired reaction temperature prior to the addition of the preheated second reactant, which is the preheated levulinic acid ester (EL or ML).

Tables 1 and 2 show the experimental matrix for the LA esterification by methanol and ethanol, respectively, while Tables 3 and Table 4 show the experimental matrix for the alkaline saponification reaction of ML and EL. The initial concentration of LA and the one of the esters are different in the sets of experiments. It was not possible to use the same initial LA concentration (LA_0) values while performing the saponifications because ML and EL are not totally soluble in water, thus a lower concentration for them has been considered.

For both esterification and saponification, the operating conditions were varied for reaction temperature, catalyst, reactant, and product initial concentrations to develop robust kinetic model.

For esterification experiments, the maximum reaction temperature was linked to the vapor pressure of the most volatile reactant species, which is the alcohol. To minimize evaporation, tt was decided that the vapor pressure should be lower than 1 bar, leading to a maximum temperature of 80 °C for ethanol and 60 °C for methanol. The minimum reaction temperature was linked to the kinetics of esterification. For ethanol esterification experiments, the kinetics was too slow when the reaction temperature was lower than 50 °C, and for methanol experiments, this minimum reaction temperature was found to be 30 °C. By using different alcohol, this temperature range could vary.

For both esterification and saponification reactions, some experiments (Run 1E & 11E, Run 2M & 3M, 5SE & 14SE and 6SM & 13SM) have been replicated to confirm the repeatability of the experiments.

Table 1. Experimental matric for LA esterification by ethanol with initial concentrations.

Run	T (°C)	H_2SO_4 (mol/L)	EL_0 (mol/L)	LA_0 (mol/L)	$EtOH_0$ (mol/L)	W_0 (mol/L)
1E	60	0.09	0.00	2.33	9.21	10.28
2E	60	0.04	0.00	2.33	9.23	10.30
3E	50	0.09	0.00	2.33	9.23	10.72
4E	80	0.04	0.00	2.33	9.23	9.22
5E	70	0.04	0.00	3.33	6.83	11.58
6E	50	0.07	0.00	2.69	8.06	11.05
7E	80	0.04	0.00	3.37	6.72	11.79
8E	80	0.07	0.00	2.23	8.88	10.92
9E	70	0.00	0.00	3.41	6.82	11.84
10E	60	0.09	0.07	2.25	8.99	10.85
11E	60	0.09	0.00	2.28	9.09	10.93
12E	70	0.09	0.00	3.39	6.78	11.80
13E	50	0.04	0.00	2.31	9.23	10.93
14E	80	0.09	0.00	2.67	8.02	11.23
15E	50	0.09	0.00	2.76	8.29	11.35

Table 2. Experimental matrix for LA esterification by methanol with initial concentrations.

Run	T (°C)	H_2SO_4 (mol/L)	LA_0 (mol/L)	$MeOH_0$ (mol/L)	ML_0 (mol/L)	W_0 (mol/L)
1M	40	0.10	2.30	9.20	0.00	20.7
2M	50	0.10	2.30	9.20	0.00	20.2
3M	50	0.10	2.30	9.20	0.00	20.3
4M	40	0.10	2.16	16.96	0.00	3.9
5M	50	0.05	2.32	9.23	0.00	20.3
6M	50	0.05	2.16	16.94	0.00	3.4
7M	40	0.10	1.00	1.00	0.00	46.7
8M	60	0.10	0.80	0.82	0.00	47.9
9M	30	0.01	2.02	11.98	0.00	16.5
10M	50	0.09	0.98	4.00	0.20	39.6
11M	40	0.09	1.39	9.12	0.30	25.8
12M	30	0.07	1.84	5.71	0.28	31.3
13M	50	0.07	1.45	0.00	0.75	46.1
14M	50	0.10	1.50	0.00	0.75	46.0

Table 3. Experimental matrix for EL saponification with initial concentrations.

Run	T (°C)	EL_0 (mol/L)	$NaOH_0$ (mol/L)	W_0 (mol/L)
1SE	40	0.30	0.30	52.23
2SE	30	0.30	0.30	52.41
3SE	20	0.30	0.30	52.58
4SE	60	0.30	0.30	51.91
5SE	30	0.10	0.10	54.24
6SE	60	0.10	0.10	51.91
7SE	70	0.10	0.10	53.60
8SE	40	0.20	0.40	52.93
9SE	40	0.20	0.20	53.17
10SE	30	0.20	0.10	53.45
11SE	40	0.20	0.10	53.28
12SE	50	0.20	0.10	53.12
13SE	50	0.10	0.10	53.80
14SE	30	0.10	0.10	54.27

Table 4. Experimental matrix for ML saponification with initial concentrations.

Run	T (°C)	ML_0 (mol/L)	$NaOH_0$ (mol/L)	W_0 (mol/L)
1SM	40	0.30	0.30	52.23
2SM	30	0.30	0.30	52.41
3SM	20	0.30	0.30	52.58
4SM	60	0.30	0.30	51.91
5SM	30	0.10	0.10	54.24
6SM	50	0.10	0.10	51.91
7SM	70	0.10	0.10	53.60
8SM	40	0.20	0.40	52.93
9SM	40	0.20	0.20	53.17
10SM	30	0.20	0.10	53.45
11SM	40	0.20	0.10	53.28
12SM	50	0.20	0.10	53.12
13SM	50	0.10	0.10	53.80
14SM	30	0.10	0.10	54.27

2.3 Analytical methods

GC-FID was used to measure the concentration of EL and ML in the esterification reactions. The apparatus is a Scion 436 GC equipped with a flame ionization detector, an autosampler, and a capillary column (ZB5, 30 m x 0.32 mm x 0.25 µm). Helium (99.99%) was the carrier gas used at a constant flow rate of 1.2 mL min^{-1} to transfer the sample from the injector, through the column, and into the FID-detector. The temperature of the injector and the detector were set at 250°C, while the program temperature of the oven was as follows: from 50°C (1 min) to 200°C (1 min) at 20°C min^{-1}. The injection volume was 1 µL and the split ratio was 1:20. During the esterification reaction, different samples were collected and diluted with acetone up to a dilution factor of 10000. In this way, a very low concentration of H_2SO_4 was present in the GC column, avoiding any damage. To evaluate the EL and ML concentration in samples, calibration curves were done between 0 mg L^{-1} to 100 mg L^{-1} of the two esters.

Concerning the saponification reactions, the hydroxide ion concentration was quantified over time following the conductivity values through a conductivity device. At first, the Eco Titrator from Metrohm was used to titrate three samples of the NaOH aqueous solution by using a 0.1 M aqueous solution of HCl. The same was done by titrating against an aqueous solution of 0.001M of HCl three samples of reaction mixture at the final reaction time. For each saponification, the value of the conductivity was recorded every 15 seconds. This titration procedure was carried out before and after the reaction to quantify the hydroxide ion concentration. By knowing the values of [OH-] and the correspondent value for the conductivity at the initial and final time it was possible to obtain the amount of OH- for every conductivity value measured during the reaction time by using the formula below:[53,54]

$$[\boldsymbol{OH_i^-}] = ([\boldsymbol{OH_n^-}] - [\boldsymbol{OH_0^-}]) * \left(\frac{\boldsymbol{K_0 - K_i}}{\boldsymbol{K_0 - K_n}}\right) + [\boldsymbol{OH_0^-}] \quad (4)$$

Eqn (4) is the hydroxonium ion concentration

where:

- $\boldsymbol{OH_i^-}$ is the hydroxonium ion concentration at time t
- $\boldsymbol{OH_n^-}$ is the final hydroxonium ion concentration
- $\boldsymbol{OH_0^-}$ is the initial hydroxonium ion concentration
- $\boldsymbol{K_0}$ is the initial conductivity value
- $\boldsymbol{K_i}$ is the conductivity value at a generic time
- $\boldsymbol{K_n}$ is the final conductivity value

2.4 Kinetic modeling

Athena Visual Studio was used to solve the ordinary differential and algebraic equations and estimate kinetic and equilibrium parameters. This software uses Bayesian inference to analyze the estimated parameters. The ordinary and algebraic equations were solved simultaneously by using the DDAPLUS package via a damped Newton method, while the GREGLUS package could provide optimal parameter estimates with 95% confidence intervals expressed by the highest probability density (HPD). GREGPLUS also provided the normalized parameter covariance matrix.[55]

Experiments were carried out in isothermal conditions. Material balances was included in Supplementary Information.

From a previous article,[56] we demonstrated that the rate of esterification can be expressed as

$$\mathbf{r}^{\mathbf{W}}_{\mathbf{esterification}} = \mathbf{k}^{\mathbf{W}}_{\mathbf{c}} * \frac{[\mathbf{H_3O^+}]}{[\mathbf{H_2O}]} * \left([\mathbf{LA}] * [\mathbf{ROH}] - \frac{\mathbf{1}}{\mathbf{K}^{\mathbf{W}}_{\mathbf{c}}} * [\mathbf{RL}] * [\mathbf{H_2O}]\right) \quad (5)$$

$\mathbf{k}^{\mathbf{W}}_{\mathbf{c}}$ is the rate constant and $\mathbf{K}^{\mathbf{W}}_{\mathbf{c}}$ is the equilibrium constant of esterification. The term w is to indicate that these constants were estimated in water solvent.

The equilibrium constant can be derived from a Van't Hoff expression

$$\ln \frac{\mathbf{K(T)}}{\mathbf{K(T_{ref})}} = \frac{-\Delta \mathbf{H^o_r}}{\mathbf{R}} \left(\frac{\mathbf{1}}{\mathbf{T}} - \frac{\mathbf{1}}{\mathbf{T_{ref}}}\right) \quad (6)$$

where, $\mathbf{K(T)}$ and $\mathbf{K(T_{ref})}$ are the equilibrium constants at a temperature T and a reference temperature; $\mathbf{\Delta H^o_r}$ is the reaction enthalpy, and R is the universal gas constant.

The concentration of hydroxonium ion $[\mathbf{H_3O^+}]$ in water solvent can be calculated as:

$$[\mathbf{H_3O^+}] = \frac{\mathbf{1}}{\mathbf{2}} * [\mathbf{H_2SO_4}]_0 + \sqrt{\frac{[\mathbf{H_2SO_4}]_0^2}{4} + \mathbf{2} * \mathbf{K_{II}} * [\mathbf{H_2SO_4}]_0 * [\mathbf{H_2O}] + \mathbf{K_{III}} * [\mathbf{H_2O}] * [\boldsymbol{RCOOH}]} \quad (7)$$

where, $[\mathbf{H_2SO_4}]_0$ is the initial concentration of sulfuric acid; $\mathbf{K_{II}}$ is the second dissociation of sulfuric acid and $\mathbf{K_{III}}$ is the carboxylic acid dissociation (Table S1 in SI). Eqn (7) was used to calculate the concentration of hydroxonium ion during the modeling.

A modified Arrhenius equation was used to estimate the rate constant:[57]

$$\ln(\mathbf{k_c(T)}) = \left[\ln(\mathbf{k_c(T_{ref})}) + \frac{\mathbf{E_a}}{\mathbf{R \cdot T_{ref}}} \cdot \left(\mathbf{1} - \frac{\mathbf{T_{ref}}}{\mathbf{T}}\right)\right] \quad (8)$$

Using Eqn (8) decreases the correlation between the rate constant and activation energy. The modified Arrhenius equation was preferred to the Eyring equation because the transmission coefficient in Eyring equation could be challenging to estimate.

To sum up, during the modeling of esterification reaction, the following kinetic and thermodynamic constants were estimated: $\ln(\mathbf{k_c(T_{ref})})$, $\mathbf{E_a}/\mathbf{R \cdot T_{ref}}$, $\ln \mathbf{K(T_{ref})}$ and $\frac{\Delta \mathbf{H^W_r}}{\mathbf{R \cdot T_{ref}}}$. The concentration of alkyl levulinate (methyl or ethyl levulinate) was used as an observable.

For saponification experiments, the reaction is irreversible. Thus, the reaction rate was expressed as

$$\mathbf{r}^{\mathbf{W}}_{\mathbf{saponification}} = \mathbf{k}^{\mathbf{W}}_{\mathbf{c}} * [\mathbf{RL}] * [\mathbf{OH^-}] \quad (9)$$

The concentration of hydroxide was used as an observable. The same approach was used for the rate constant, and the following constants were estimated $\ln(\mathbf{k_c(T_{ref})})$ and $\frac{\mathbf{E_a}}{\mathbf{R \cdot T_{ref}}}$.

The objective function to minimize by GREGPLUS was: $\boldsymbol{OF} = (\boldsymbol{C_{exp}} - \boldsymbol{C_{estimated}})^2$.

3 Results and discussion

For clarity, different phenomenological results are present in Supplementary Information (Figures S1 to S14).

3.1 Experimental results

As shown in the experimental matrix (Tables 1-4), some experiments were performed twice to ascertain the repeatability of the data (Figures S1&S2 and Figures S9&S10) for both systems. Temperature effect (Figures S3&S4 and Figures S11&S12), catalyst effect (Figures S7&S8) and molar ratio effect ROH/Carbo and NaOH/ester (Figures S5&S6 and Figures 13&14) were also investigated. These experiments confirm that the increase in temperature, catalyst and molar ratio increases the kinetics of the reaction.

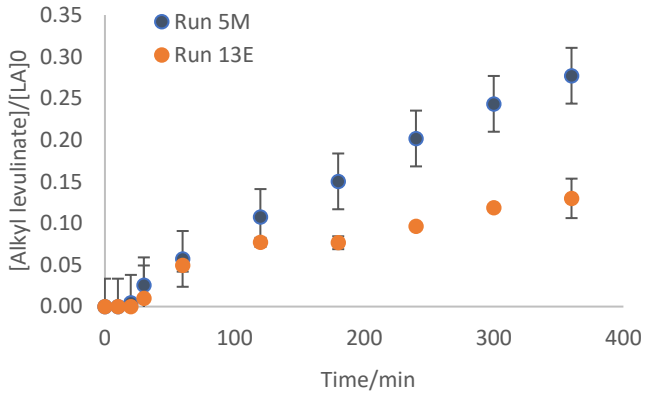

Fig. 4 Normalized ML and EL concentration with time for the esterification at 50 °C and 0.05 M of sulfuric acid, where the error bars are the standard deviation of repeated measurements.

Fig. 4 shows the normalized concentration of the two esters synthesized over time by comparing Run 5M and Run 13E, conducted at the same operating conditions. The kinetics of LA esterification by methanol is faster than that by ethanol. Indeed, the methanol molecule is smaller than ethanol, thus more reactive. In the same way, Fig. 5 depicts the decrease in the normalized ester concentration over time for two saponification reactions conducted at the same operating conditions.

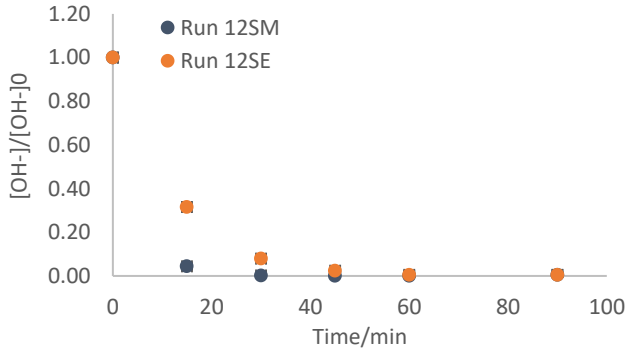

Fig. 5 Normalized ML and EL with time for the saponification at 50 °C and initial concentration of NaOH of 0.3M, where the error bars are the standard deviation of repeated measurement.

Fig. 5 confirms that the saponification of ML is faster than EL. One can also observe that the saponification reaction is irreversible.

The kinetic modeling for each saponification and esterification was developed using Athena Visual Studio. Kinetic and thermodynamic constants (eqns (6) and (8)) were estimated at a reference temperature. These values are summarized in Tables 5&6. Kinetic constants for the esterification of levulinic acid by ethanol in water solvent were obtained in a previous work.[58] Parity plots and normalized covariance matrices were displayed in SI.

The normalized covariance matrices (Tables S2, S3, S4 and S5) show that the parameters were well-identified, because no values were higher than 0.95 and lower than -0.95 between the estimated parameters.[58] Parity plots (Figures S15, S16, S17 and S18) show that developed models can well predict experimental concentrations. Indeed, the coefficient of determination (R^2) is higher than 0.90 in each case. From Tables 4 and 5, credible intervals measured by the 95% marginal highest posterior density intervals were low, showing the high precision of the estimated constants.

Figs 6 & 7 illustrate the rate constant evolution for LA esterification by methanol and ethanol and for ML and EL saponification with temperature. A temperature range of [20 – 50]°C was considered. This temperature range was choosen based on the experimental matrix (Tables 1-4) in order to have a safe margin of errors for the evaluation of Taft substituent parameters. The mean estimated values are obtained from $\boldsymbol{ln\left(k_c^W(T_{ref})\right)}$ and $\frac{E_a^W}{R \cdot T_{ref}}$ (Tables 5 and 6). The colored area represents the credible intervals, which are the 95% marginal HPD intervals.

Fig. 6 shows that the credible interval for ethanol is larger than for methanol, because the estimate constant credible intervals for LA esterification by methanol are slightly shorter. One can observe that the rate constant for methanol and ethanol (mean values) are relatively similar in the temperature range of 20-30 °C.

Fig. 6 shows that the credible intervals for ML saponification are slightly larger than for EL saponification. One can observe that there is no overlapping for both rate constants, and the rate constant for ML saponification is the highest one.

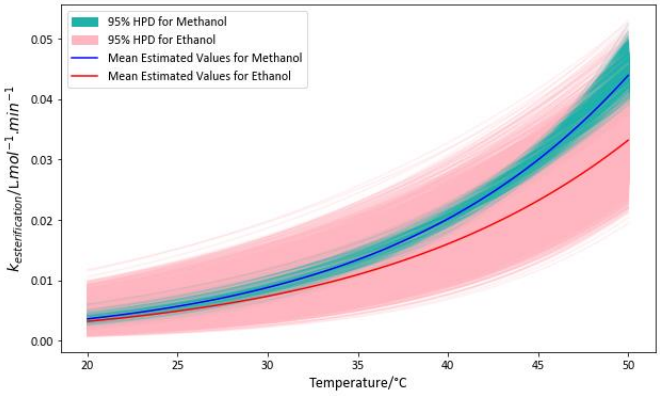

Fig. 6 Rate constant evolution for LA esterification by methanol and ethanol with temperature.

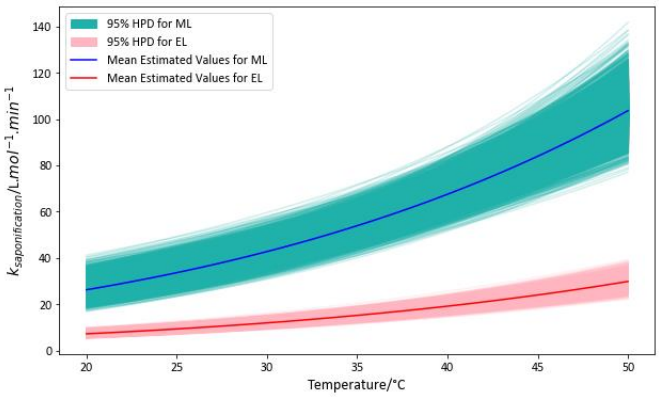

Fig. 7 Rate constant evolution for ML and EL saponification with temperature.

Table 5. Estimated parameters for ML and EL esterification at a reference temperature.

	T_{ref} (°C)		Units	Estimated value	95% marginal HPD intervals
ML	44.2	$ln(k_c^W(T_{ref}))$	L.mol^{-1}.min^{-1}	-3.57	0.03
		$\frac{E_a^W}{R \cdot T_{ref}}$	-	24.78	1.72
		$ln(K_c^W(T_{ref}))$	-	1.87	0.23
		$\frac{\Delta H_r^W}{R \cdot T_{ref}}$	-	27.14	12.11
EL	64.0	$ln(k_c^W(T_{ref}))$	L.mol^{-1}.min^{-1}	-2.46	0.08
		$\frac{E_a^W}{R \cdot T_{ref}}$	-	21.82	2.42
		$ln(K_c^W(T_{ref}))$	-	1.14	0.18
		$\frac{\Delta H_r^W}{R \cdot T_{ref}}$	-	18.18	5.80

Table 6. Estimated parameters for ML and EL saponification at a reference temperature.

	T_{ref} (°C)		Units	Estimated value	95% marginal HPD intervals
ML	42.0	$ln(k_c^W(T_{ref}))$	L.mol^{-1}.min^{-1}	4.30	0.07
		$\frac{E_a^W}{R \cdot T_{ref}}$	-	13.76	1.28
EL	41.7	$ln(k_c^W(T_{ref}))$	L.mol^{-1}.min^{-1}	3.03	0.07
		$\frac{E_a^W}{R \cdot T_{ref}}$	-	14.24	0.74

Once the kinetic and thermodynamic constants have been evaluated, the Taft substituent parameters have been recalculated in a temperature range of [20-50] °C, by following eqns 2 and 3. The evolution of the steric and polar effects was displayed by Figs 8 and 9. The value of Es and σ* is zero for methyl group because it is the reference one. The circles (Figs 8 and 9) were calculated using the estimated kinetics constants values in Tables 5 and 6, and one can observe that the temperature effect is relatively low on both parameters.

For the ethyl group, both substituent Taft parameters vary linearly with the temperature but with an antagonist effect.

In Fig. 8, the dependence of Es towards temperature is more significant than for σ* (coefficient of determination of -0.0022 $°C^{-1}$ compared to 0.0011). The temperature increase leads to a decrease of Es from -0.056 at 20°C to -0.126 at 50°C, meaning that the steric hindrance increases within this temperature range. This increase in steric hindrance from the ethyl group can be linked to the increase of its mobility with temperature. As the temperature increases, the free energies of the transition states associated with the different possible conformations tends to favour a higher Boltzmann population of the sterically more hindered isomers, where states with lower energy always have a higher probability of being occupied than the ones with higher energy. On the contrary, the value of σ^*increases from -0.203 at 20°C to -0.167 at 50°C (Fig. 9), meaning that the substituent polar effect decreases with temperature. One should keep in mind that σ^* describes the field and inductive effect of the substituent. The tabulation of data points from Figs 8 and 9 can be found in Table S6.

Fig. 8 Taft steric substituent values for ethyl group with temperature.

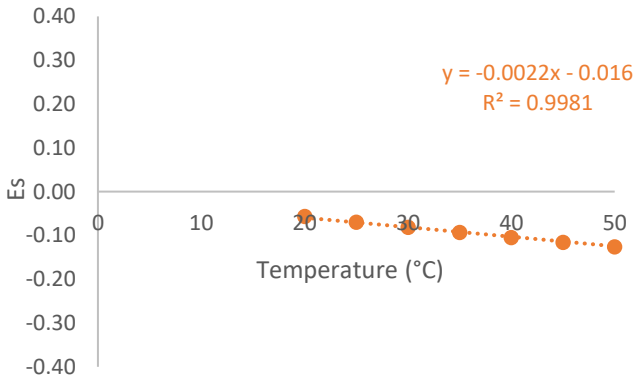

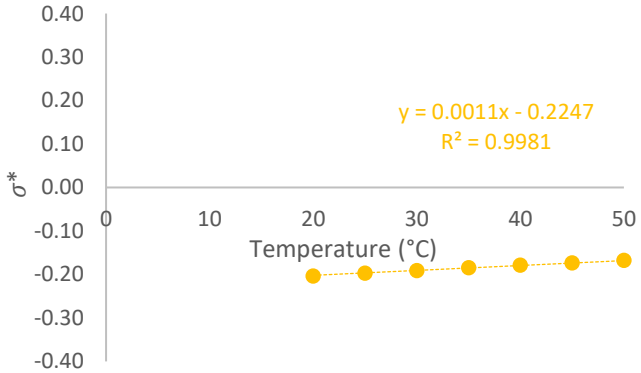

Fig. 9 Taft polar substituent values for MeOH and EtOH with temperature.

The Taft substituent parameters were determined initially at 25°C,[22] and the value of Es was re-estimated at 40°C.[36] Table 7 compares the values obtained in this study with the ones found in the literature. At 25°C, the Es value obtained by Taft and our study is very similar, but for σ^* the value obtained by Taft is two times lower than ours. At 40 °C, the values obtained by MacPhee et al.[36] and ours are similar. The differences can be due to the fact that we separated the contribution of the hydroxonium concentration and considered the reversibility on the rate of esterification (eqn (4)).

Table 7. Polar and steric effects at 25°C and 40°C.

	T (°C)	Es, calc	Es, lit	σ^*, calc	σ^*, lit
Ethyl	25	-0.065	-0.070[18]	-0.199	-0.10[18]
Ethyl	40	-0.099	-0.08[36]	-0.180	Not found

Conclusions

In this article, we evaluated the impact of temperature on the Taft substituent parameters for the polar (σ*) and the steric (Es) contribution of the methyl group. Kinetic models were developed for the esterification of levulinic acid by methanol and ethanol catalyzed by sulfuric acid, and the saponification of methyl levulinate and ethyl levulinate by sodium hydroxide. Experiments were carried out in isothermal conditions. The developed models fit well the experimental concentration, the estimated parameters were well-identified and low-correlated.

From these estimated kinetic constants, it was found that polar and steric Taft parameters of the ethyl group vary linearly within the temperature range 20 to 50 °C. The value of σ* varies from -0.205 at 20 °C to -0.169 at 50°C; and the value of Es varies from -0.052 at 20°C to -0.122 at 50°C. The sensitivity towards temperature was higher for Es than for σ*. In this temperature range, the increase of temperature increases the steric effect and lowers the polar effect.

An effort was done to include the uncertainty, characterized by the 95% credible intervals of the estimated kinetic constants, on the polar and steric Taft parameters. Using our kinetic models, the uncertainty decreases when temperature increases, within the temperature range 20-50°C.

This work uses robust kinetic models to show the importance of reaction temperature on σ* and Es values of the ethyl groups. A deeper investigation could be carried out with quantum mechanics to better understand the temperature effect of Taft substituent parameters. Another continuation of this work is the effect of this variation on the Taft reaction parameters, i.e., ρ* and δ.

Acknowledgements

The authors thank INSA Rouen Normandy, University of Rouen Normandy, the Centre National de la Recherche Scientifique (CNRS), European Regional Development Fund (ERDF) N◦ HN0001343, Labex SynOrg (ANR-11-LABX-0029), Carnot Institute I2C, the graduate school for reasearch XL-Chem (ANR-18-EURE-0020 XL CHEM) and Region Normandie for their support. GC/FID was financed by ERDF RIN Green Chem 2019NU01FOBC08 N◦ 17P04374.

This research was funded, in whole or in part, by the ANR (French National Research Agency) and the DFG (German Research Foundation) through the project MUST (MicroflUidics for Structure-reactivity relationships aided by Thermodynamics & kinetics) [ANR-20-CE92-0002-01 - Project number 446436621].

Notes and references

1 S. Takkellapati, T. Li and M. A. Gonzalez, *Clean Technol. Environ. Policy*, 2018, **20**, 1615–1630.
2 J. G. de Vries, *Curr. Opin. Green Sustain. Chem.*, 2023, 39, 100715.
3 S. Wang, A. Cheng, F. Liu, J. Zhang, T. Xia, X. Zeng, W. Fan and Y. Zhang, *Ind. Chem. Mater.*, 2023, **1**, 188–206.
4 K. Guo, Q. Guan, J. Xu and W. Tan, *J. Bioresour. Bioprod.*, 2019, 4, 202–213.
5 G. Li, W. Liu, C. Ye, X. Li and C. L. Si, *Int. J. Polym. Sci.*, , DOI:10.1155/2018/4723573.
6 D. M. Alonso, S. G. Wettstein, M. A. Mellmer, E. I. Gurbuz and J. A. Dumesic, *Energy Environ. Sci.*, 2013, **6**, 76–80.
7 D. Di Menno Di Bucchianico, Y. Wang, J. C. Buvat, Y. Pan, V. Casson Moreno and S. Leveneur, *Green Chem.*, 2022, 24, 614–646.
8 G. W. Huber, A. Lapkin and N. Yan, *React. Chem. Eng.*, 2020, 5, 2131–2133.
9 M. G. Evans and M. Polanyi, *Trans. Faraday Soc.*, 1936, 32, 1333–1360.
10 M. G. Evans and M. Polanyi, *Trans. Faraday Soc.*, 1935, **31**, 875–894.
11 M. G. Evans and M. Polanyi, *Trans. Faraday Soc.*, 1938, **34**, 11–24.
12 L. P. De Oliveira, D. Hudebine, D. Guillaume and J. J. Verstraete, *Oil Gas Sci. Technol.*, 2016, **71**, 45.
13 A. Verloop, W. Hoogenstraaten and J. Tipker, in *Drug Design*, Elsevier, 1976, pp. 165–207.
14 A. Verloop, in *Pesticide Chemistry: Human Welfare and Environment*, Pergamon, 1983, pp. 339–344.
15 K. C. Harper, E. N. Bess and M. S. Sigman, *Nat. Chem.*, 2012, 4, 366–374.
16 L. Rummel, M. H. J. Domanski, H. Hausmann, J. Becker and P. R. Schreiner, *Angew. Chemie - Int. Ed.*, 2022, **61**, e202204393.
17 L. P. Hammett, *Trans. Faraday Soc.*, 1938, 34, 156–165.
18 R. W. Taft, *Steric Effects in Organic Chemistry*, Wiley, New York, USA, 1956.
19 R. W. Taft, *J. Am. Chem. Soc.*, 1953, **75**, 4534–4537.
20 R. W. Taft, *J. Am. Chem. Soc.*, 1953, **75**, 4231–4238.
21 R. W. Taft, *J. Am. Chem. Soc.*, 1953, **75**, 4538–4539.
22 R. W. Taft, *J. Am. Chem. Soc.*, 1952, **74**, 3120–3128.
23 R. W. Taft, *J. Am. Chem. Soc.*, 1952, **74**, 2729–2732.
24 M. Charton, *J. Org. Chem.*, 1976, **41**, 2217–2220.
25 M. Charton, *J. Am. Chem. Soc.*, 1975, **97**, 1552–1556.
26 M. Charton, *J. Am. Chem. Soc.*, 1975, **97**, 3691–3693.
27 M. Charton, *J. Org. Chem.*, 1968, **33**, 3878–3882.
28 E. S. C. Kwok and R. Atkinson, *Atmos. Environ.*, 1995, **29**, 1685–1695.
29 E. Grosjean, D. Grosjean, M. P. Fraser and G. R. Cass, *Environ. Sci. Technol.*, 1996, **30**, 2687–2703.
30 D. Grosjean and E. L. Williams, *Atmos. Environ. Part A, Gen. Top.*, 1992, **26**, 1395–1405.
31 C. Hansch, A. Leo and R. W. Taft, *Chem. Rev.*, 1991, **91**, 165–195.
32 A. F. Zahrt, S. V. Athavale and S. E. Denmark, *Chem. Rev.*, 2020, 120, 1620–1689.
33 O. Said-Aizpuru, F. Allain, A. Dandeu, F. Diehl, D. Farrusseng and J. F. Joly, *React. Chem. Eng.*, 2021, **6**, 1079–1091.
34 L. P. Hammett, *J. Am. Chem. Soc.*, 1937, **59**, 96–103.
35 Z. Lan and Y. Lu, *React. Chem. Eng.*, 2022, **7**, 833–838.
36 J. A. MacPhee, A. Panaye and J. E. Dubois, *Tetrahedron*, 1978, **34**, 3553–3562.
37 J. E. Dubois, J. A. Macphee and A. Panaye, *Tetrahedron*, 1980, **36**, 919–928.
38 A. Panaye, J. A. MacPhee and J. E. Dubois, *Tetrahedron*, 1980, **36**, 759–768.
39 A. Brändström, *J. Chem. Soc. Perkin Trans. 2*, 1999, 1855–1857.
40 K. Neuvonen, H. Neuvonen, A. Koch and E. Kleinpeter, *Comput. Theor. Chem.*, 2012, **981**, 52–58.
41 A. Sahu and A. B. Pandit, *Ind. Eng. Chem. Res.*, 2019, **58**, 2672–2682.
42 J. Vojtko and P. Tomčík, *Int. J. Chem. Kinet.*, 2014, **46**, 189–196.
43 J. Lilja, D. Y. Murzin, T. Salmi, J. Aumo, P. Maäki-Arvela and M. Sundell, *J. Mol. Catal. A Chem.*, 2002, **182**–**183**, 555–563.
44 A. A. Issa, M. El-Azazy and A. S. Luyt, *Sci. Rep.*, , DOI:10.1038/s41598-019-54095-0.
45 S. Leveneur, D. Y. Murzin and T. Salmi, *J. Mol. Catal. A Chem.*, 2009, **303**, 148–155.
46 S. Leveneur, *Org. Process Res. Dev.*, 2017, **21**, 543–550.

47 Y. Wang, M. Cipolletta, L. Vernières-Hassimi, V. Casson-Moreno and S. Leveneur, *Chem. Eng. J.*, 2019, **374**, 822–831.
48 Z. Xue, D. Yu, X. Zhao and T. Mu, *Green Chem.*, 2019, **21**, 5449–5468.
49 Z. Yu, X. Lu, J. Xiong and N. Ji, *ChemSusChem*, 2019, 12, 3915–3930.
50 C. Antonetti, D. Licursi, S. Fulignati, G. Valentini and A. M. R. Galletti, *Catalysts*, 2016, 6, 196.
51 L. Yan, Q. Yao and Y. Fu, *Green Chem.*, 2017, **19**, 5527–5547.
52 F. D. Pileidis and M. M. Titirici, *ChemSusChem*, 2016, 9, 562–582.
53 M. K. A. Mesfer, *Int. J. Chem. React. Eng.*, , DOI:10.1515/ijcre-2016-0174.
54 K. Das, P. Sahoo, M. Sai Baba, N. Murali and P. Swaminathan, *Int. J. Chem. Kinet.*, 2011, **43**, 648–656.
55 W. E. Stewart and M. Caracotsios, *Computer-Aided Modeling of Reactive Systems*, 2007.
56 S. Baco, M. Klinksiek, R. Ismail Bedawi Zakaria, E. Antonia Garcia-Hernandez, M. Mignot, J. Legros, C. Held, V. Casson Moreno and S. Leveneur, *Chem. Eng. Sci.*, 2022, **260**, 117928.
57 G. Buzzi-Ferraris, *Catal. Today*, 1999, **52**, 125–132.
58 K. Toch, J. W. Thybaut and G. B. Marin, *AIChE J.*, 2015, **61**, 880–892.